# The Effect of the Primary Solvate Shell on the Mechanism of the Stöber Silica Synthesis. A Density Functional Investigation

**Péter Terleczky and László Nyulászi***

*Department of Inorganic and Analytical Chemistry, Budapest University of Technology and Economics, H-1111 Budapest Szt. Gellért tér 4, Hungary*

*Received: July 29, 2008; Revised Manuscript Received: November 4, 2008*

The target of the present computational study was the acid catalyzed bond cleavage of the Si−O and C−O bonds in siloxane, alkoxysilane and ether in aqueous media. In the present study the effect of water as a solvent has been modeled using a full primary solvate shell built up from water molecules connected via hydrogen bonds around the reacting molecules. The interaction energy between the embedding water cluster and the "solvated" molecule gives an estimate for solution effects. The cleavage of the Si−O bonds in these molecular clusters proceeds with low barriers; furthermore the reaction energies corrected with the solvent interaction energies gives a reaction thermodynamics, which is in accordance with the experimental results. Molecules with a Si−O bond form stable pentavalent silicon with the solvent water molecules if protonated, while in the case of the neutral molecules tetracoordinate silicon is obtainable. The summary of the calculated reaction paths gives a possible route of siloxane formation from methoxysilane in aqueous media. The same computational methodology predicts that the hydrolysis of dimethyl ether is hindered by a substantial barrier.

## Introduction

The preparation of colloidal silicon dioxide particles from alkoxysilanes (usually tetraethoxysilane, TEOS) in aqueous media (the Stöber method[1]) is a widely used procedure. There are two fundamental steps in this reaction: (i) the hydrolysis of a carbon−oxygen−silicon bond leading to silanol and alcohol; (ii) the condensation of two silanol units resulting in a new siloxane (silicon−oxygen−silicon) bond. The entire procedure is either acid or base catalyzed:

$$R_3E^1-O-E^2R'_3 + H_2O \leftrightarrow R_3E^1-OH + R'_3E^2-OH$$

$$E^1, E^2: C, Si$$

The hydrolysis of the siloxane bond in acidic media has also been observed in the case of siloxane oligomers[2,3] and in a slow process even for quartz.[4] However, usually the condensation of silanols takes place. This is in contrast with the behavior of the ether (carbon−oxygen−carbon) bond, which is known to hydrolyze under harsh reaction conditions only (high temperature and solid catalyst) in an $S_N2$ type reaction.[5] The hydrolysis reaction has been studied in order to produce methanol, which is decomposed by steam reformation to carbon monoxide and hydrogen (and other byproducts). This method is believed to serve as a green path to produce a hydrogen-rich feed for fuel cells.[6] There have been several attempts, both experimental[7] and theoretical,[8] to determine the mechanism of the hydrolysis of the Si−O bond. Early kinetic studies[2] have indicated that in the acid catalyzed reaction a complex containing three or four water molecules is involved. While no further experimental data have been reported, quantum chemical studies were performed to study the hydrolysis of the silicon−oxygen bond for both siloxane[8−10] and alkoxysilane[11] bond systems. The transition structures obtained were significantly (by 11 kcal/mol 6-311+g(2d,p)//HF/6-31g*[8]) stabilized due to the formation of a complex with four water molecules connected by hydrogen bonds. To our best knowledge no such calculations have been carried out for the silicon−oxygen−carbon bond system. However, all computations reported so far have failed to give a thermodynamically acceptable reaction pathway. A likely reason for this failure is that the solvent effect has not properly been considered, and the presence of further water molecules can alter the relative energies.

The aim of this work was to find an adequate model, and use it in order to provide a proper description of the full reaction route in a cost-effective way. The main problem with the implicit models, which consider the solvent via an external potential field, is that they lack interfacial interactions.[12] Furthermore the previous studies mentioned above have also indicated the explicit involvement of water molecules in the reaction.

An obvious approach is to embed the dissolved target molecules in a solvent cluster. In order to have a computationally tractable system we use here water instead of ethanol. Both the structure and the stability of various water clusters (with 8 to 20 monomer units[13]) have been investigated in detail. Calculations of clusters consisting of 48, 123 and 293 water molecules have also been reported,[14] showing the feasibility of this approach. All the stable clusters have some common properties: they contain linear (or near to linear) hydrogen bonds, and the "surface" of the cavernous clusters is formed from water pentamers or hexamers (pentagons and hexagons respectively). By using cluster models many known properties of bulk water can be described. For example even a water cluster modeling the autoprotolytic reaction by the presence of both oxonium and a hydroxide ion[15] has been reported.

These results have indicated that an explicit water monolayer may be useful in modeling the hydrolysis reaction. Such a model is tractable at current computational levels. It is especially noteworthy in this respect that such water clusters are known to form clathrate structures with certain small molecules, e.g. methane, chlorine[16] or alkali cations.[17] In these cases a coordinatory dodecahedral ($n = 20$) water assembly has been observed.

* Corresponding author. E-mail: nyulaszi@mail.bme.hu.

10.1021/jp8067206 CCC: $40.75 © 2009 American Chemical Society
Published on Web 01/07/2009

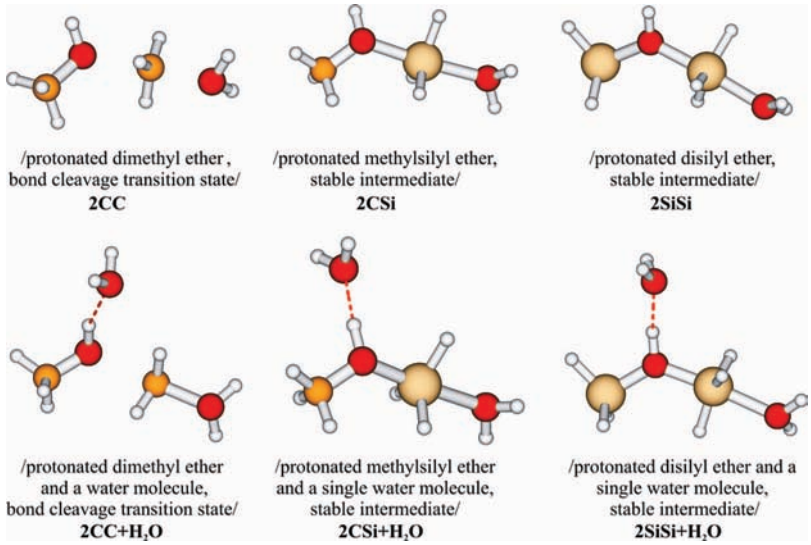


**Figure 1.** Pentavalent structures (**2EE′**) of the bond cleavage reactions summarized in Table 1.

**TABLE 1: Calculated Relative Energies (kcal/mol) for the Characteristic Stationary Points of the Ether, Alkoxysilane and Siloxane Bond Cleavage[a]**

| bond system E−O−E′ | complexing water molecules | **1EE′**, protonated ether form + $H_2O$ | **2EE′**, pentavalent structure | **3EE′**, complex of hydrolysis products |
|---|---|---|---|---|
| C−O−C | 0 | 0 (M) | 15.3 (TS) | 10.9 (M) |
| | 1 | 0 (M) | 24.7 (TS) | 23.9 (M) |
| C−O−Si | 0 | 0 (TS) | −16.0 (M) | 12.5 (TS) |
| | 1 | 0 (TS) | −13.5 (M) | 19.2 (TS) |
| Si−O−Si | 0 | 0 (TS) | −17.8 (M) | 6.4 (TS) |
| | 1 | 0 (TS) | −9.3 (M) | 18.4 (TS) |

[a] M denotes minimum, TS denotes transition structure.

## Computational Methods

All structures were fully optimized at the B3LYP/6-31G* level of theory, using the Gaussian 03 program package.[18] Geometries for hydrogen-bonded systems optimized with the B3LYP functional[19,20] have been found to be almost identical to those computed at the MP2 level of theory,[21] thus the geometry optimizations were carried out at the B3LYP/6-31G* level. Subsequent calculation of the second derivatives was carried out to characterize the nature of the stationary points obtained. The energies were improved by single point B3LYP/6-31+G*//B3LYP/6-31G* calculations, since it is likely that for a proper energetical description (of the hydrogen bonds) the use of diffuse functions is essential.[22,23] The number of water molecules in the investigated cluster was chosen to provide full coverage for the solvated molecule. The principles to form the starting geometries of the clusters were to (I) keep linear hydrogen bonds, (II) arrange the water molecules as pentamers[24] and hexamers, and (III) keep the tetrahedral structure around the oxygen of each water molecule. Full geometry optimizations were carried out from starting structures fulfilling these criteria. The use of a PCM model to account for the bulk solvent beyond the first shell has also been considered; the results showed only a slight energetic effect for the solvation energies and accordingly on the calculated reaction paths (see Supporting Information Table S1). Transition state structures were verified by subsequent optimizing after changing the geometry along the single imaginary frequency. For the visualization of the molecules, the Molden program was used.[25]

## Results and Discussion

The first step in our studies was to choose model molecules for the calculations. The smallest possible systems are disilyl ether, methyl silyl ether and dimethyl ether. These model molecules were used in previous computational studies[8−10] as well. To take into consideration the effect of the acid catalysis the protonated forms of the reagent molecules were investigated throughout,[26] and the protonation effects were investigated separately (see below).

As key points in the reaction path, we have considered the complex formed from the reactant (protonated ether) and an attacking water (**1EE′**), a pentacoordinate structure (**2EE′**) and the hydrolysis product (**3EE′**), which is the complex formed from two separate alcohol (silanol) molecules. Not only has the gas phase reaction been investigated but also the effect of a single explicit water molecule has been taken into account. This method has also been applied in previous computational investigations of the Si−O bond cleavage;[8−10] however, this is the first study to calculate all the important stationary points on the reaction path for all of the three related hydrolysis reactions at a uniform level of the theory. As expected, in the case of the ether hydrolysis the pentavalent structure (**2CC**, see Figure 1) has a single imaginary frequency, with the expected motion characteristic for an $S_N2$ type mechanism.[27,28] Furthermore this transition structure is less stable than the water complex formed with the protonated ether, which is in turn a real minimum (**1CC**, Table 1, see Supporting Information Figure S1). Replacement of at least one carbon by silicon changes the picture completely. The pentavalent structure (**2CSi** and **2SiSi**) becomes the most stable point on the reaction path,[27,28] and the complexes with water (**1CSi** and **1SiSi**) as well as the complex of the hydrolysis products (**3CSi** and **3SiSi**) are transition structures! The van der Waals complexes between water and the protonated methoxysilane, or disiloxane, could not be located on the potential energy surface, although significant effort[29] has

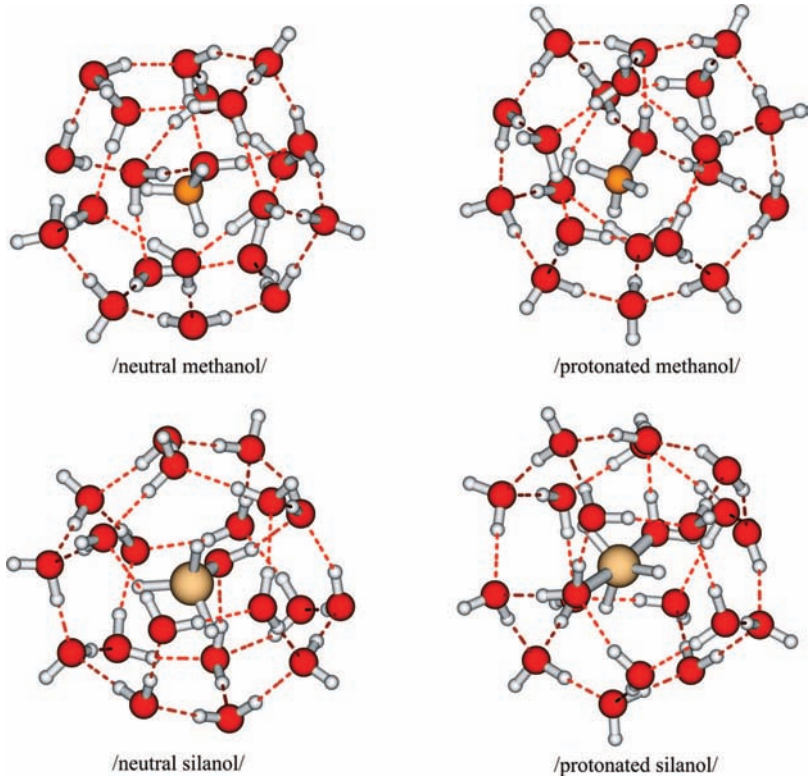


**Figure 2.** Optimized hydrate shell for the expected bond cleavage products.

been devoted to find these minima, since upon optimization always the pentavalent structure (which is the thermodynamic sink on the reaction path) has been obtained. The stability of the reactants as compared to the hydrolysis products is also noticeable. The energy of the separated alcohols resulting from the bond cleavage exceeds the energy of the reactants by 10.2 kcal/mol for the dimethyl ether, 8.7 kcal/mol for the methyl silyl ether and 7.7 kcal/mol for the disilyl ether. While this result is expected for the siloxane and the ether bond, the silicon−oxygen−carbon bond is known to cleave, thus the hydrolysis products are expected to be more stable than the reactants. The failure to describe the experimental observations is likely to be attributed to the solvent effects, which are not considered in the above computations.

The effect of one additional water molecule in stabilizing the transition structure **3SiSi** was noted before.[8] **3CSi** is also stabilized to a similar extent. Nevertheless, **2CSi** and **2SiSi** (with a pentavalent silicon) are still the most stable structures on the investigated reaction pathway. The effect of an extra water molecule on the ether hydrolysis pathway differs from that of the silicon analogues, **2CC** is even more destabilized, as a result of the interaction with the single extra water molecule. The water molecule also influences the relative stability of the products compared to the reactants. The energy of the separated "products" (with the water molecule bound to the protonated alcohol) exceeds that of the reactants by 8.8 kcal/mol for the dimethyl ether, 4.0 kcal/mol for the methyl silyl ether and 6.1 kcal/mol for the disilyl ether.

Embedding the solute molecules in a water cluster as discussed above should account for both the possible stabilizing and destabilizing interactions. The dodecahedral water cluster structure fits well to the smaller solute molecules (e.g., methanol, silanol). For the larger systems (ethers and separated alcohols/silanols as hydrolysis products) larger clusters (with 23 water molecules) were needed to provide a full coverage of the investigated system. The resulting structures for the clusters containing 20 water molecules are shown in Figure 2. The starting structure for the optimization was a dodecahedral cage, which has been deformed slightly upon optimization in the cases of neutral and more significantly in the case of protonated clusters.

The neutral clusters show analogous behavior for both methanol and silanol. The apolar, hydrophobic group ($CH_3$ and $SiH_3$) repels the solvent, and the hydroxide group interacts with the solvent shell via hydrogen bonds (see Figure 2). The C−O bond length of methanol is increased by about 0.06 Å in the solvent shell in comparison to the isolated molecule. This effect is somewhat smaller than the 0.1 Å elongation (Table 2) obtained in case of protonation (in the gas phase). On the contrary the Si−O distance remains unchanged in the solvent shell.

Upon protonation[30] the structure of the embedded molecules is getting drastically different. The proton, which was attached originally to the oxygen atom of methanol, is shifted upon optimization to the solvent shell (we were unable to locate any minima corresponding to $MeOH_2^+(H_2O)_{20}$), whereby it may migrate with low barriers. We computed several minima which differ only in the orientation of the proton in the solvate shell around methanol, and the energy difference between these structures is small (see Supporting Information Figure S2), but none of these contained two short OH distances at the methoxy oxygen. Accordingly the C−O distance in this cluster is similar to that in the neutral molecule (Table 2). Silanol, however, creates a new silicon−oxygen bond, forming a pentavalent silicon atom as it is shown in Figure 2. In this pentavalent structure the Si−O distance (Table 2) is shortened somewhat with respect to that in the gas phase form of the protonted silanole, and the Si−O (water) distance (2.054 Å) is longer than the usual Si−O bond. We were able to compute a minimum which differs only in the orientation of the proton in the solvate

shell around the hypervalent silanol, but this structure is less stable by 2.9 kcal/mol (see Supporting Information Figure S2).

While protonation of the oxygen in the isolated ether increases the C−O distance (see Figure 3 and Table 2), neither the geometry of dimethyl ether nor that of its protonated form is significantly affected in the water cluster. In the case of the pentavalent form (which is a first-order saddle point), however, the late transition structure (note that $O_1-E'$ is longer than $E'-O_2$; see Figure 4 and Table 2) becomes an early transition structure as a result of the interaction with the embedding water molecules. Contrary to this, in the pentavalent form of both the methyl silyl ether and disilyl ether the $O_1-E'$ distance remains nearly unchanged upon hydration. The $E-O_1-Si$ angle shows large changes upon hydration. This is not surprising since the Si−O−Si bond is known to be easily deformed between 120 and 180° [31−37] and the constraint posed by the embedding solvent cluster reduces the size of the molecule. It is remarkable that for the solvated neutral methyl silyl ether we were able to locate minima with both hypervalent and tetravalent silicon (**NCSih** and **NCSi**, respectively) while in the case of the disilyl ether only the structure with the hypervalent silicon (**NSiSi**) could be found. None of the carbon atoms forms an excess bond in the case of dimethyl ether with the solvent molecules (**NCC**). It is worthy to note that neither methyl silyl ether nor disilyl ether forms a stable complex with water (see Table 3).

The interaction between solvate and solute molecules not only results in structural changes but the difference of the solvation energies of the reactants, intermediates and products has a significant effect on the energetics of the reaction. Solvation energy is defined in eq 1:

$$X(H_2O)_n \xrightarrow{E_{solvation}} X + (H_2O)_n \quad (1)$$

where $X(H_2O)_n$ represents an ether solvated by $n$ water molecules, $(H_2O)_n$ is a water cluster consisting of $n$ molecules, and X is the solute without a solvent shell. The value of $n$ is 20 for the alcohols, and the oxonium ion, and 23 for the protonated and neutral ether forms. The data are summarized in Table 3.

In the case of water the data for both solvent shells ($n = 20$ and $n = 23$) are displayed. The difference between the solvation energy of the two water clusters amounts to 6.5 kcal/mol, which is roughly the energy of one hydrogen bond. It is known that clusters consisting of 20 and 24 water (containing only water pentamers, and so the maximum number of possible H-bonds) have enhanced stability.[38] Accordingly clusters consisting of 21 and 23 water molecules show some destabilization. Thus, it is also clear that the size of the water cluster is of importance, and we come back to this point later.

We have also defined a replacement energy as the energy of the following reaction (eq 2):

$$X \cdot (H_2O)_n + H_2O \xrightarrow{E_{replacement}} X + (H_2O)_{n+1} \quad (2)$$

where $X\cdot(H_2O)_n$ represents the solute solvated by $n$ water molecules, X is the solute without a solvent shell and $H_2O_{n+1}$ is a calculated minimum of a water cluster consisting of $n + 1$

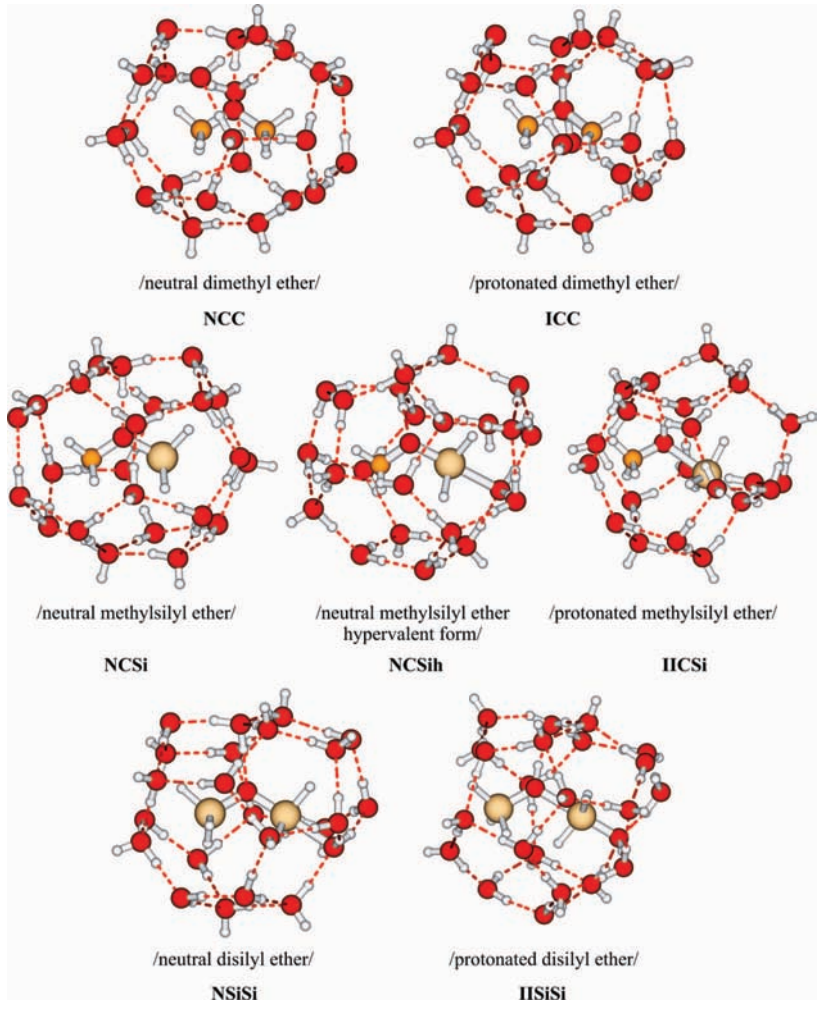


**Figure 3.** The hydrate shell created for the ether form of the reactants.

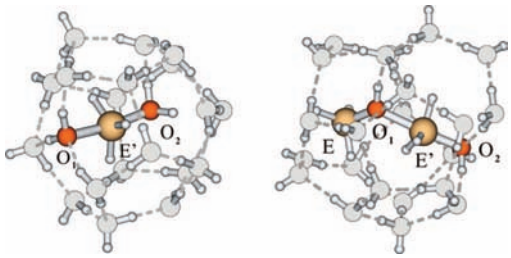


**Figure 4.** The atoms selected to follow geometric changes upon protonation and hydration.

water molecules. The replacement energies (see Table 3) differ from the solvation energies by the solvation energy of one water. The results show that all protonated ether and alcohol forms are stabilized within the hydrate shell. In the case of the (protonated) silicon containing compounds the stabilization is attributable to the formation of the hypervalent structure as discussed above. The case of methanol is also noteworthy. While the solvation energy value indicates some stabilization (methanol prefers to be dissolved in water), the replacement energy value shows that the replacement of water by methanol is a slightly endothermic process, as expected.

To check if our level of calculation is adequate, we have calculated the solvation energy defined by eq 1 for silanol and methanol (in a cluster of 20 water molecules) with different basis sets (Table 4) and functionals (see Supporting Information Table S2). The geometries used were those obtained at the B3LYP/6-31g* level of theory. As it has been noted before,[39] the diffuse functions are essential to describe hydrogen bonds. From the present results (Table 4) it seems that this statement holds for the small basis sets, and the results at 6-31+G* are close to the aug-cc-PVTZ values, while the cc-PVDZ values differ from those significantly. Interestingly, the HF solvation energies are similar for silanol to those obtained by the different functionals using DFT methods, while for methanol the clusters are much less stabilized (see Supporting Information Table S2).

Further calculations have been carried out to check the effect of size of the water cluster. As model molecule we have chosen the neutral methanol, and clusters consisting of 19 to 23 water molecules were investigated. Each cluster was considered as the sum of three layers: the solvated molecule (methanol) in the center, a primary solvate shell (molecules with no other water molecules between them and the methanol) and a secondary shell the members of which only had direct H-bond contact with molecules of the primary shell and/or each other. The number of water molecules in the primary shell determines the size of the cavity in which the solute is embedded. Each starting geometry for these optimizations contained the maximum number of hydrogen bonds between the water molecules of the primary and the secondary shell.

We have calculated a solvation energy per water molecule (eq 3), to compare the stability obtained by the formation of each cluster:

$$CH_3OH \cdot (H_2O)_n \xrightarrow{n \cdot E_{\text{solvation per water molecule}}} CH_3OH + nH_2O \quad (3)$$

where $CH_3OH \cdot (H_2O)_n$ represents a methanol solvated by a cluster consisting of $n$ water molecules. Our concept was to create a primary hydrate shell only; the cage that fulfills the previous criteria is the one consisting of 20 water molecules. This cluster has a deformed dodecahedral structure, the deformation due to the hydrogen bonds formed with the embedded solute. The value of calculated solvation energy per water molecule is an almost constant value, showing that neither increasing the primary solvation shells' size (indicated as $N_{\text{cavity}}$ in Table 5) nor the addition of elements of the secondary shell provides a better result.

While the solvation energies for a single water molecule are nearly constant, the replacement energy has a minimum at $n = 20$ (see Table 6). Since methanol is unrestrictedly soluble in water, we expect that the replacement energy is quite low; by our interpretation this means that the system shows only little difference on the replacement of a single molecule. The cluster with the second lowest replacement energy is the one containing a monolayer of 20 water molecules. Only the shell containing a cavity of 19 water molecules, and consisting of a sum of 20 water molecules, shows a slightly better result, but the optimized cluster does not cover the methanol perfectly: the excess water molecule in the secondary shell "pulls" the primary shell so that it opens up at the methyl group. Again neither increasing the primary solvate shells' size nor the buildup of the secondary shell provides a better result.

Before turning to the energetics of the investigated reactions, it should be noted that protonation has significant energetic consequences, and this should be taken into consideration in

**TABLE 2: The Effect of Protonation and Hydration on Bond Lengths and Angles**

| | gaseous phase | | | | with hydrate shell | | | |
|---|---|---|---|---|---|---|---|---|
| species | E−$O_1$ (Å) | $O_1$−E′ (Å) | E′−$O_2$ (Å) | E−$O_1$−E′ (deg) | E−$O_1$ (Å) | $O_1$−E′ (Å) | E′−$O_2$ (Å) | E−$O_1$−E′ (deg) |
| neutral methanol | | 1.418 | | | | 1.472 | 3.388 | |
| protonated methanol | | 1.522 | | | | 1.439 | 3.231 | |
| neutral silanol | | 1.666 | | | | 1.667 | 3.233 | |
| protonated silanol | | 1.868 | | | | 1.849 | 2.054 | |
| neutral dimethyl ether | 1.410 | 1.410 | | 112.2 | 1.424 | 1.418 | 3.251 | 112.9 |
| protonated dimethyl ether | 1.484 | 1.484 | | 122.9 | 1.465 | 1.466 | 3.052 | 114.4 |
| protonated dimethyl ether, bond cleavage transition state | 1.449 | 2.066 | 1.871 | 118.4 | 1.433 | 1.894 | 1.980 | 113.5 |
| neutral methyl silyl ether | 1.419 | 1.660 | | 122.1 | 1.438 | 1.674 | 3.281 | 118.2 |
| neutral methyl silyl ether, hypervalent form | | | | | 1.424 | 1.740 | 2.206 | 113.1 |
| protonated methyl silyl ether | 1.492 | 1.824 | | 126.4 | | | | |
| protonated methyl silyl ether, hypervalent form | 1.467 | 1.952 | 2.052 | 123.5 | 1.440 | 2.156 | 1.769 | 114.4 |
| neutral disilyl ether | 1.652 | 1.652 | | 141.4 | 1.664 | 1.747 | 2.213 | 116.6 |
| protonated disilyl ether | 1.822 | 1.822 | | 130.9 | | | | |
| protonated disilyl ether, hypervalent form | 1.769 | 1.948 | 2.067 | 129.5 | 1.702 | 2.207 | 1.767 | 119.9 |

**TABLE 3: Calculated Solvation Energies (Eq 1) and Replacement Energies (Eq 2)**

| species | solvation energy (kcal/mol) | replacement energy (kcal/mol) |
|---|---|---|
| protonated dimethyl ether | 32.1 | 18.7 |
| protonated methyl silyl ether | 37.5 | 24.1 |
| protonated disilyl ether | 31.8 | 18.4 |
| neutral dimethyl ether | −11.8 | −25.2 |
| neutral methyl silyl ether | −20.0 | −33.4 |
| neutral methyl silyl ether (hypervalent) | −19.9 | −33.3 |
| neutral disilyl ether | −29.9 | −43.3 |
| neutral methanol | 1.8 | −5.2 |
| protonated methanol | 56.4 | 49.5 |
| neutral silanol | −19.6 | −26.6 |
| protonated silanol | 49.9 | 42.9 |
| oxonium ion | 81.5 | 74.6 |
| water ($n = 21$) | 6.9 | |
| water ($n = 24$) | 13.4 | |

**TABLE 4: Calculated Solvation Energies (kcal/mol) for the Methanol and Silanol Depending on Method and Basis Set**

| method: | B3LYP | | BLYP | |
|---|---|---|---|---|
| basis set | methanol | silanol | methanol | silanol |
| 6-31g* | 9.7 | −15.8 | 9.5 | −18.4 |
| 6-31+g* | 3.0 | −18.5 | 1.3 | −21.8 |
| 6-31++g* | 3.3 | −18.0 | 1.6 | −21.3 |
| 6-311+g** | 2.0 | −18.0 | 0.1 | −21.5 |
| cc-PVDZ | 15.0 | −12.5 | 15.6 | −25.9 |
| aug-cc-PVDZ | 3.9 | −15.6 | 2.5 | −7.6 |
| cc-PVTZ | 4.8 | −17.3 | 3.8 | −20.4 |
| aug-cc-PVTZ | 1.1 | −18.5 | | |

**TABLE 5: Calculated Solvation Energies (kcal/mol) per Water Molecule for Methanol, Depending on the Size and Structure of the Surrounding Cluster (See Eq 3)**

| $N_{cavity}$: | 19 | 20 | 21 | 22 | 23 |
|---|---|---|---|---|---|
| $N_{summa}$ | | | | | |
| 19 | 11.8 | | | | |
| 20 | 11.8 | 11.8 | | | |
| 21 | 11.8 | 11.9 | 12.0 | | |
| 22 | 11.7 | 11.9 | 11.9 | 11.9 | |
| 23 | 11.8 | 11.8 | 12.0 | 11.8 | 11.5 |

**TABLE 6: Calculated Replacement Energies (Eq 2, kcal/mol) of Methanol, Depending on the Size and Structure of the Surrounding Cluster**

| $N_{cavity}$: | 19 | 20 | 21 | 22 | 23 |
|---|---|---|---|---|---|
| $N_{summa}$ | | | | | |
| 19 | 9.4 | | | | |
| 20 | 4.4 | 5.1 | | | |
| 21 | 12.6 | 9.3 | 8.2 | | |
| 22 | 12.3 | 9.1 | 9.2 | 8.2 | |
| 23 | 11.4 | 11.2 | 8.5 | 8.5 | 19.4 |

the understanding of the reactivity, thus the energy of protonation should be investigated on the solvated molecules. Equation 4 provides an estimate for the protonation energy in aqueous media:

$$X \cdot (H_2O)_n + H^+ \cdot (H_2O)_m \xrightarrow{E_{protonation}} XH^+ \cdot (H_2O)_n + (H_2O)_m \quad (4)$$

where $XH^+ \cdot (H_2O)_n$ and $X \cdot (H_2O)_n$ represents a protonated and the neutral ether solvated by $n$ water molecules, respectively ($n$ is set to 23 as discussed above). $(H_2O)_m$ and $H^+ \cdot (H_2O)_m$ are a water cluster and a protonated water cluster consisting of $m$ molecules ($m$ is set to 20 as discussed above). The respective protonation energies are 8.7 kcal/mol for the dimethyl ether, −6.8 kcal/mol for the methyl silyl ether and −4.8 kcal/mol for the siloxane. Thus, the protonation of the ether is endothermic, and the protonation of the silicon containing analogues is exothermic.

The results obtained for the hydrolysis reaction of dimethyl ether embedded in water molecules are shown in Scheme 1. Likewise in the case of the gas phase reaction, the process is of $S_N2$ type. The protonation energy displayed was obtained from eq 4. The energy level **NCC**, which was set to 0 kcal/mol, represents the reactant side of the reaction: the neutral ether in its solvent shell. **ICC** is the protonated ether, **IICC** is the transition state of the bond cleavage, and **IIICC** denotes the products sharing the original solvate shell of the reactant. These latter three states are analogous with **1CC**, **2CC** and **3CC**, and the Roman numerals indicate that the target molecules are in the solvent shell. The calculated activation barrier (21.6 kcal/mol) is not too high. However, the protonation of the ether is also endothermic, contributing by another 8.7 kcal/mol to the barrier of the entire reaction. Also we could optimize the protonated form (at the oxygen) of the ether embedded in the solvate shell of 23 water molecules, and this structure turned out to be more stable than **ICC** by 16.2 kcal/mol. Also the transition structure for the proton shift to the ether is only 0.1 kcal/mol less stable than **ICC**, showing that no kinetic hindrance can be expected for the proton shift in the solvate shell. Although the C−O bond cleavage of **ICC** cannot be ruled out, the small concentration of the protonated form blocks the reaction path.

To characterize energetically the formation of the products (methanol and protonated methanol, each in its own solvate shell) we made use of the replacement energies (Table 3). This shows that the products solvated in separate shells (each surrounded by 20 water molecules, **IVCC**) are favored by 17.3 kcal/mol compared to **IIICC**. In summary, the bond cleavage of ether is possible, but only under rather harsh reaction conditions—in agreement with the experimental results, due to the unfavored formation of the protonated ether and the reaction barrier.

In the following we discuss the hydrolysis reaction of the methyl silyl ether (Scheme 2) and that of disilyl ether (Scheme 3).

The **NCSi** structure represents the neutral methyl silyl ether within a water cluster of 23 molecules. The next state, **IICSi**, is the protonated methyl silyl ether within a solvate shell containing a pentavalent silicon. This state is analogous with **2CSi**, our efforts to find a structure analogous to **1CSi** have failed. This finding is similar to our observation in the case of the protonated silanol optimized within the solvent shell. A further minimum where the excess proton is at the solvate shell is less stable than **IICSi** (by 6.5 kcal/mol). The transition structure (by 16.4 kcal/mol above **IICSi**) corresponding to the protonation of the methyl silyl ether allows a facile reaction. The transition state for the bond cleavage is **IIICSi**, and the hydrolysis products within the solvate shell of 23 water molecules are marked by **IVCSi**.

To understand the fate of the separated methanol and silanol obtainable from **IVCSi** we made again use of the calculated replacement energies (Table 3) for the products (neutral methanol and protonated silanol—being stabilized by the formation of the pentavalent silicon structure, each within its own solvate shell consisting of 20 water molecules, **VCSi**). The products in the separate shells are favored by 12.4 kcal/mol.

**SCHEME 1: Calculated Reaction Path for the Hydrolysis of the Dimethyl Ether, with a Full Primary Solvate Shell**[a]

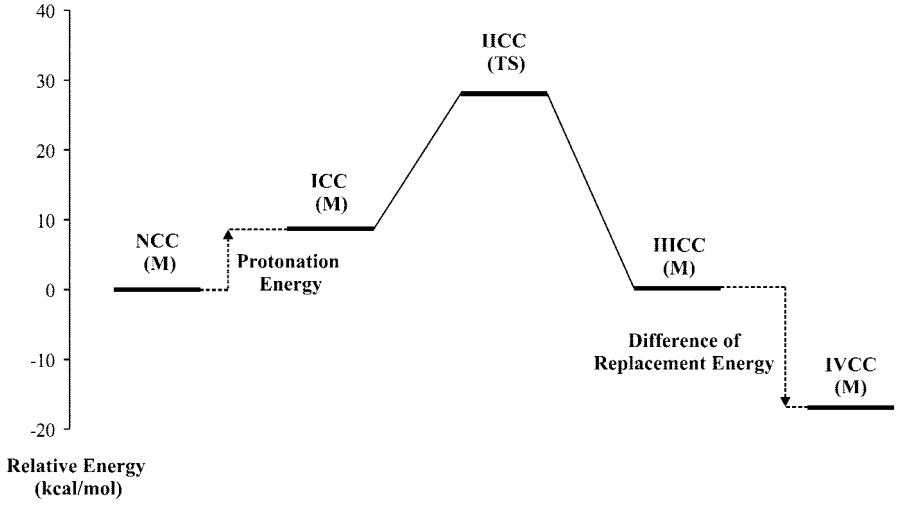


[a] M denotes minimum, TS denotes transition state.

**SCHEME 2: Calculated Reaction Paths for the Hydrolysis of the Methyl Silyl Ether, with a Full Primary Solvate Shell**[a]

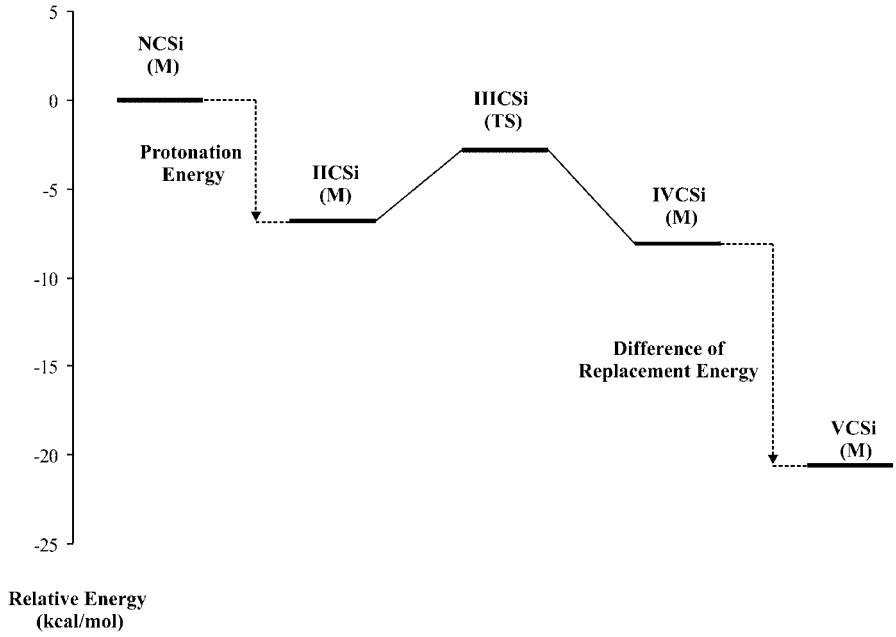


[a] M denotes minimum, TS denotes transition state.

The energy difference of **IICSi** and **IVCSi** is small, and they are separated by a low barrier. This reaction is therefore determined by the thermodynamics, i.e. the formation and the further reaction of the hydrolysis products (in their dissolved form).

Scheme 3 displays the bond cleavage reaction path for disilyl ether. The neutral siloxane form is the starting point of the reaction (**NSiSi**). The protonation energy is exothermic by 4.8 kcal/mol, leading to the protonated form **IISiSi**. A further minimum, where the proton is located in the solvate shell, is unfavored compared to **IISiSi** by 3.1 kcal/mol. The barrier leading from this structure to **IISiSi** is only 3.0 kcal/mol. Again the Roman numerals indicate the solvated analogues of the structures calculated in gaseous phase. Likewise in the case of the methyl silyl ether, we were unable to find a solvated structure similar to **1SiSi**. Therefore it is likely that in aqueous solutions the siloxanes favor a pentavalent structure upon protonation, which forms instantly and without any significant barrier. The transition state for the cleavage of the SiOSi bond is **IIISiSi**. It is worthy to note that the cyclic, hydrogen-bonded complex consisting of four water molecules and the cleaving SiOSi unit suggested by Apeloig and co-workers for this transition state[8] can be clearly recognized in **IIISiSi** (Figure 5). Such a network can also be recognized in Figure 5 for the transition state structures of the bond cleavage of dimethyl ether (**IICC**) and methyl silyl ether (**IIICSi**).

The products, two silanols (neutral and protonated), are in a common cavity of 23 water molecules (**IVSiSi**). The replacement energy (Table 3) gain if each of the two product molecules is placed in a separate shell consisting of 20 water molecules (**VSiSi**) is slightly (by 1.8 kcal/mol) endothermic.

The energetics of the calculated hydrolysis path shows that it is rather a bond condensation. Though the protonated siloxane (**IISiSi**) is the most stable among the displayed structures, the barrier that separates it from **IVSiSi** is low. Furthermore the stability difference between siloxane and silanol (and protonated silanol) is small. Thus, the equilibrium can easily be shifted by the formation of siloxane oligomers by the condensation of more

**SCHEME 3: Calculated Reaction Paths for the Hydrolysis of the Disilyl Ether with a Full Primary Solvate Shell[a]**

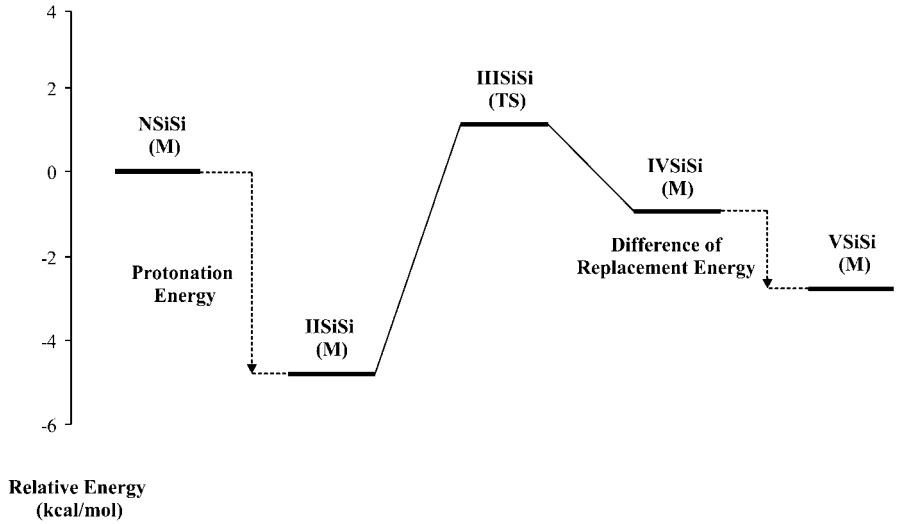


[a] M denotes minimum, TS denotes transition state.

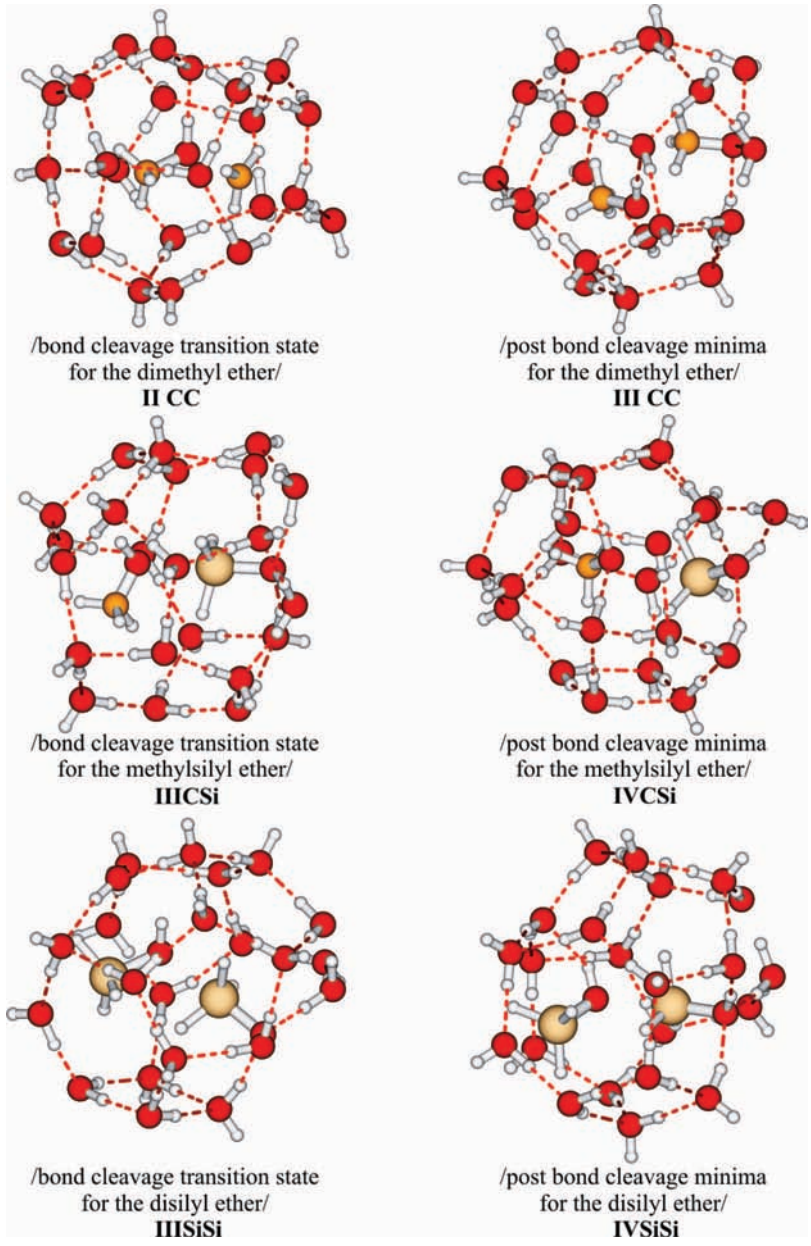


**Figure 5.** The bond cleavage transition states and the bond cleavage products sharing the same hydrate shell.

silanols. Such an oligomer would provide an apolar environment, to which the next silanol molecule can bind to with a further energy gain. Accordingly, silanols are known to form siloxane bonds in acidic conditions.[40]

## Conclusions

The mechanism of the acid catalyzed hydrolysis of dimethyl ether, methoxysilane and disiloxane has been studied computationally in aqueous media. The effect of the solvent has been modeled using a full primary solvate shell built up from water molecules connected via hydrogen bonds. While for the smaller molecules (methanol and silanol) 20 molecules of water provide a full coverage, for ether, methyl silyl ether and disiloxane 23 water molecules are needed. The interaction energy between solvent and solute can be obtained via different schemes, the most reliable one being the replacement energy, where the energy of the replacement of the solute by a single water in the cluster is considered. In the protonated clusters silicon is always pentavalent, being connected to an oxygen atom of one of the water molecules. Accordingly, these structures are significantly stabilized in the solvate shell. While ether is destabilized in the water cluster by protonation, and this together with the $S_N2$ type barrier hinders the hydrolysis, in the case of the silicon containing compounds the protonation is stabilizing. Since the reaction barriers are low for both methyl silyl ether and disiloxane, these hydrolytic reactions are controlled by the thermodynamics. While in the case of methyl silyl ether the bond cleavage is favored energetically (resulting in methanol and a hypervalent protonated silanol), in the case of the siloxane the bond cleavage is energetically disfavored, when using the present model to account for the solvent effect. All these results are in accordance with the experimental observations, indicating that the applied microsolvation model is reliable.

**Acknowledgment.** Financial support from the Hungarian Scientific Foundation OTKA T 049258 is gratefully acknowledged.

**Supporting Information Available:** Complete ref 18, Figure S1 of nonpentavalent key structures of the bond cleavage reaction in the gaseous phase and with a single complexing water molecule, Figure S2 of alternative protonated hydrate structures of methanol and silanol, Table S1 on the effect of a PCM model on calculated reaction energies for the bond cleavage reaction in the protonated clusters, Table S2 on the effect of functionals and basis set and Tables S3−S66 of optimized structures in Cartesian coordinate format. This material is available free of charge via the Internet at http://pubs.acs.org.

## References and Notes

(1) Stöber, W.; Fink, A.; Bohn, E. *J. Colloid Interface Sci.* **1968**, *26* (1), 62–69.
(2) Wilczek, L.; Chojnowski, J. *Macromolecules* **1981**, *14*, 9–17.
(3) Chuit, C.; Corriu, R. J. P.; Reye, C.; Young, J. C. *Chem. Rev.* **1993**, *93*, 1371–1448.
(4) de Leeuw, N. H.; Higgins, F. M.; Parker, S. C. *J. Phys. Chem. B* **1999**, *103*, 1270–1277.
(5) Polydore, C.; Roundhill, M.; Liu, H. *J. Mol. Catal. A: Chem.* **2002**, *186*, 65–68.
(6) Semelsberger, T. A.; Borup, R. L. *J. Power Sources* **2005**, *152*, 87–96.
(7) Schmidt, H.; Schloze, H.; Kaiser, A. *J. Non-Cryst. Solids* **1984**, *63*, 1–11.
(8) Cypryk, M.; Apeloig, Y. *Organometallics* **2002**, *21*, 2165–2175.
(9) Kudo, T.; Gordon, M. S. *J. Am. Chem. Soc.* **1998**, *120*, 11432–11438.
(10) Kudo, T.; Gordon, M. S. *J. Phys. Chem. A* **2000**, *104*, 4058–4063.
(11) Okumoto, S.; Fujita, N.; Yamabe, S. *J. Phys. Chem. A* **1998**, *102*, 3991–39988.
(12) Cramer, C. J.; Truhlar, D. G. *Chem. Rev.* **1999**, *99*, 2161–2200.
(13) Maheshwary, S.; Patel, N.; Sathyamurthy, N.; Kulkarni, A. D.; Gadre, S. R. *J. Phys. Chem. A* **2001**, *105*, 10525–10537.
(14) Kazimirski, J. K.; Buch, V. *J. Phys. Chem. A* **2003**, *107*, 9762–9775.
(15) Kuo, J.-L.; Ciobanu, C. V.; Ojamäe, L.; Shavitt, I.; Singer, S. J. *J. Chem. Phys.* **2003**, *118*, 3583–3588.
(16) Pauling, L.; Marsh, R. E. *Proc. Natl. Acad. Sci. U.S.A.* **1952**, *38*, 112–118.
(17) Tanaka, M.; Aida, M. *J. Solution Chem.* **2004**, *33*, 887–901.
(18) Frisch, M. J.; *Gaussian 03, Revision C.02*; Gaussian, Inc.: Wallingford, CT, 2004.
(19) Becke, A. D. *J. Chem. Phys.* **1993**, *98*, 5648.
(20) Lee, C.; Yang, W.; Parr, R. G. *Phys. Rev. B* **1988**, *37*, 785.
(21) Santra, B.; Michaelides, A.; Scheffler, M. *J. Chem. Phys.* **2007**, *127*, 184104.
(22) Pudzianowski, A. T. *J. Phys. Chem.* **1996**, *100*, 4781–4789.
(23) Novoat, J. J.; Sosa, C. *J. Phys. Chem.* **1995**, *99*, 15837–15845.
(24) Lenz, A.; Ojamäe, L. *Phys. Chem. Chem. Phys.* **2005**, *7*, 1905–1911.
(25) Schaftenaar, G.; Noordik, J. H. *J. Comput.-Aided Mol. Des.* **2000**, *14*, 123–134.
(26) The energetic consequences of protonation in solution will be discussed below.
(27) Bento, A. P.; Bickelhaupt, F. M. *J. Org. Chem.* **2007**, *72*, 2201–2207.
(28) Pierrefixe, S. C. A. H.; Guerra, C. F.; Bickelhaupt, F. M. *Chem. Eur. J.* **2008**, *14*, 819.
(29) We have applied different optimization strategies, including selection of reduced stepsize, calculation of second derivatives at the initial point of the optimization etc.
(30) In case of a 1 M proton concentration 55 water molecules are present for one proton, thus the 20−23 water clusters correspond to a ca. 2 M acid concentration.
(31) Ribeiro-Claro, P. J. A.; Amado, A. M. *J. Mol. Struct. (THEOCHEM)* **2000**, *528*, 19.
(32) Tielens, F.; Proft, F. D.; Geerlings, P. *J. Mol. Struct. (THEOCHEM)* **2001**, *542*, 227.
(33) Csonka, G. I.; Réffy, J. *Chem. Phys. Lett.* **1994**, *229*, 191.
(34) Csonka, G. I.; Erdõsy, M.; Réffy, J. *J. Comput. Chem.* **1994**, *15*, 925.
(35) Bakk, I.; Bóna, Á.; Nyulászi, L.; Szieberth, D. *J. Mol. Struct. (THEOCHEM),* **2006**, *770*, 111.
(36) Koput, J. *Chem. Phys.* **1990**, *148*, 299.
(37) Koput, J. *J. Mol. Spectrosc.* **1993**, *160*, 143.
(38) Ludwig, R.; Appelhagen, A. *Angew. Chem., Int. Ed.* **2005**, *44*, 811–815.
(39) Pan, Y.; McAllister, M. A. *J. Mol. Struct. (THEOCHEM)* **1998**, *427*, 22l–227.
(40) Chojnowski, J.; Cypryk, M.; Kaźmierski, K.; Rózga, K. *J. Non-Cryst. Solids* **1990**, *125*, 40–49.

JP8067206